6-4-2012

The effects of diameter and chirality on the thermal transport in free-standing and supported carbon-nanotubes

Bo Qiu
Purdue University, qiub3@purdue.edu

Yan Wang
Purdue University, yanwang@purdue.edu

Xiulin Ruan
Birck Nanotechnology Center, Purdue University, ruan@purdue.edu

Qing Zhao
Purdue University, zhao172@purdue.edu

Qiu, Bo; Wang, Yan; Ruan, Xiulin; and Zhao, Qing, "The effects of diameter and chirality on the thermal transport in free-standing and supported carbon-nanotubes" (2012). *Birck and NCN Publications.* Paper 1174.
http://dx.doi.org/10.1063/1.4725194

AIP | Applied Physics Letters

The effects of diameter and chirality on the thermal transport in free-standing and supported carbon-nanotubes

Bo Qiu, Yan Wang, Qing Zhao, and Xiulin Ruan

Citation: Appl. Phys. Lett. **100**, 233105 (2012); doi: 10.1063/1.4725194
View online: http://dx.doi.org/10.1063/1.4725194
View Table of Contents: http://apl.aip.org/resource/1/APPLAB/v100/i23
Published by the AIP Publishing LLC.

The effects of diameter and chirality on the thermal transport in free-standing and supported carbon-nanotubes

Bo Qiu, Yan Wang, Qing Zhao, and Xiulin Ruan[a)]
School of Mechanical Engineering and the Birck Nanotechnology Center Purdue University West Lafayette, Indiana 47907-2088, USA

(Received 16 January 2012; accepted 17 May 2012; published online 5 June 2012)

We use molecular dynamics simulations to explore the lattice thermal transport in free-standing and supported single-wall carbon-nanotube (SWCNT) in comparison to that in graphene nanoribbon and graphene sheet. For free-standing SWCNT, the lattice thermal conductivity increases with diameter and approaches that of graphene, partly due to the curvature. Supported SWCNT thermal conductivity is reduced by 34%-41% compared to the free-standing case, which is less than that in supported graphene. Also, it shows an evident chirality dependence by varying about 10%, which we attribute to chirality-dependent interfacial phonon scattering. © *2012 American Institute of Physics*. [http://dx.doi.org/10.1063/1.4725194]

Carbon-nanotube (CNT) and graphene nanoribbon (GNR) have attracted lots of attention since the last decade due to their promising electronic, mechanical, and thermal properties, as suggested by various experimental[1–3] and theoretical studies.[4,5] Recent experiments on synthesizing GNRs from unzipping CNTs (Ref. 6) have proved their close relation. Both single-wall CNTs (SWCNTs) and GNRs can be characterized by chirality. It was found that both the electrical resistivity of SWCNT and the elastic and electrical properties of GNR are strongly dependent on chirality.[7–9] In contrast, the thermal conductance was only found to strongly depend on chirality and edge types in GNR (Refs. 10 and 11) but not in free-standing CNTs.[10,12] The mechanisms responsible for such difference in the chirality dependent lattice thermal transport are not yet clear. On the other hand, reduction in thermal conductivity has been experimentally demonstrated in supported graphene.[13] Theories were proposed to explain such observation[14,15] and suggest similar reduction in supported CNT.[16,17] However, the importance of chirality and diameter on the lattice thermal conductivity of supported SWCNT remains unknown. In this work, we use non-equilibrium molecular dynamics (NEMD) simulations to study the lattice thermal conductivity of free-standing and supported SWCNT with various diameters then compare to GNR and single-layer graphene sheet (SLG). We find interesting diameter dependence in free-standing CNT and identify the relation of the thermal transport in CNT to that in GNR. We also report the chirality dependence of thermal conductivity in supported CNTs. Furthermore, our findings suggest supported CNTs may be advantageous for planar heat dissipation applications.

Since the electrons in CNT/GNRs only have limited contributions to total thermal conductivity,[18] they are not the main concern of this paper. All classical molecular dynamics (MD) simulations are carried out using the LAMMPS package.[19] The C-C interactions within GNR, SLG, and CNT are modeled using optimized Tersoff potential (OPT), which is made to provide better description of anharmonicity and phonon dispersions than existing classical potentials for carbon-based systems.[20] SiO_2 is modeled after Munetoh[21] while the interactions between CNT and substrate, namely C-Si and C-O, are assumed to be van der Waals[22] and modeled using Lennard-Jones (LJ) potential

$$V(r_{ij}) = 4\epsilon\left[\left(\frac{\sigma}{r_{ij}}\right)^{12} - \left(\frac{\sigma}{r_{ij}}\right)^{6}\right], \tag{1}$$

with parameters $\epsilon_{C-Si} = 8.909\,\text{meV}$, $\sigma_{C-Si} = 3.629\,\text{Å}$, $\epsilon_{C-O} = 3.442\,\text{meV}$ and $\sigma_{C-O} = 3.275\text{Å}$ for C-Si and C-O interactions, respectively.[23] The cutoffs for LJ interactions are taken as 2.7σ.

The geometries studied include free-standing GNR (and SLG), half-rolled GNR, CNT, and CNT on SiO_2 substrate, as shown in Fig. 1. Free boundary conditions (FBC) are applied in all directions for all cases except for the width direction of SLG where periodic boundary conditions (PBC) are used. The last columns of atoms at the two ends in the

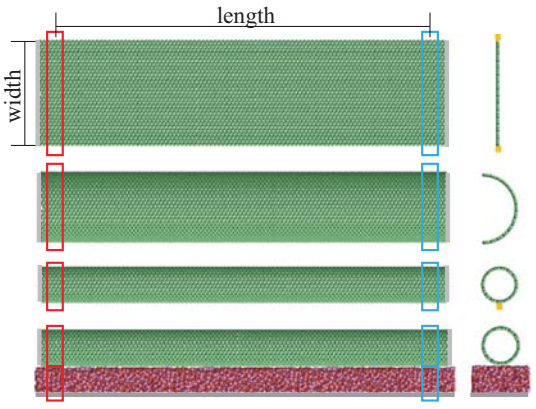

FIG. 1. From top to bottom: the MD domains for free-standing GNR (or SLG when boundaries in width direction are set to be periodic), half-rolled GNR, free-standing CNT, and CNT supported on SiO_2 substrate. Colored lines at the boundaries: orange represents free or fixed rows of atoms; gray represents fixed atoms. Red and blue boxes represent hot and cold thermal baths. Cross-sectional views are shown on the right.

[a)]ruan@purdue.edu.

length direction are fixed to prevent atoms from sublimating. No current leakage through these fixed ends is found. For free-standing cases, two thermal baths of 1 nm width each are used at the two ends with temperature controlled by direct velocity scaling.[24] Wider thermal baths and lower velocity scaling frequency are not found to affect the thermal conductivity noticeably. For supported cases, we prepare amorphous SiO_2 following the heating-quenching recipe[25] then cut out a block with length, width, and thickness equal with 2.5 nm, 3.6 nm, and 2.0 nm, respectively. The block is duplicated in the length direction to match the length of CNTs and equilibrated under FBC for 1 ns with bottom 0.5 Å layer fixed. Similar thicknesses of SiO_2 substrate were used in previous CNT/SLG-substrate thermal studies.[15,16] CNT is released from 1.6 Å above the substrate then run in constant temperature and volume ensemble (NVT) with FBC for 2 ns to allow for interfacial structure relaxation and thermal equilibration. Four thermal baths are used for supported cases (Fig. 1) to ensure local temperature match at the interfaces to minimize interfacial heat flux.

The timestep used for free-standing and supported cases are 0.8 fs and 0.4 fs, respectively. Ten independent simulations are run for each case to minimize statistical fluctuations. All cases are first run in NVT for 400 ps to equilibrate at 300 K. Temperatures of 330 K and 270 K are then designated in the thermal baths at the two ends to create temperature gradient and heat flux. Simulations are run for another 3 ns to ensure steady-state and then the linear regions of the temperature profiles along length direction are extracted to obtain the temperature gradient dT/dx. Thermal conductivity κ_l is obtained according to Fourier's law of heat conduction

$$\kappa_l = -\frac{J/A}{dT/dx}. \tag{2}$$

Here A is the effective cross-sectional area, which is taken as the cross-sectional perimeter times the graphene thickness 3.35 Å for CNT, GNR, and SLG. The heat current J is computed as

$$J = t_s^{-1} \sum \Delta E, \tag{3}$$

where $\sum \Delta E$ is the accumulated energy change in thermal baths due to velocity scaling and t_s is the total time during which temperature control is applied.[24]

First of all, we study the thermal conductivity of free-standing CNT with different diameter D in comparison to corresponding GNR and SLG. κ_l of CNT is found to monotonically increase with increasing tube length L and does not appear to saturate at a length of 400 nm, similar to that of GNR. To allow for clean comparison, we obtain κ_l in bulk limit by fitting to $1/\kappa_l - 1/L$ relation under gray approximation and extrapolating to $L \to \infty$,[26,27] where excellent linear correlation is found, as illustrated in the inset of Fig. 2.

As seen in Fig. 2, κ_l of CNT is lower than but approaches that of SLG as D increases from 0.7 ((5,5) and (9,0) CNTs) to 2.9 nm ((21,21) and (36,0) CNTs). This observation opposes findings from some previous studies, which suggested that κ_l decreases with diameter and κ_l of SLG serves as lower limit.[28–30] Nonetheless, our observed trend for CNT with moderate diameters does agree with that from the exact solution of phonon Boltzmann transport equation (BTE) reported in Ref. 31, where OPT was also used. The absence of a thermal conductivity minimum at very small diameters in our simulations is likely due to the fully anharmonic description of out-of-plane phonons in MD.[14] Since OPT was made to improve the description of anharmonicity and phonon dispersions in CNT/graphene, the observed inconsistency with some of the past literature is likely due to this improvement. To justify, we also simulate a-CNTs using original Tersoff potential[32] under otherwise same simulation conditions, where consistency with previous studies is found (Fig. 2). Therefore, the use of OPT does account for the different trend.

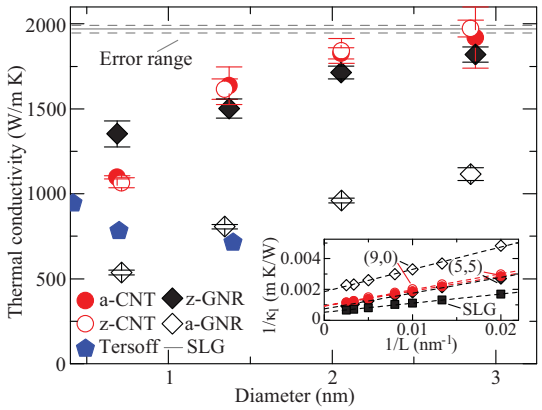

FIG. 2. Thermal conductivities of CNTs, GNRs, and SLG extrapolated to bulk limit. GNR width $w = \pi D$. Also shown are CNT thermal conductivity obtained using original Tersoff potential. The prefixes "a-" and "z-" represent armchair and zigzag, respectively. Inset: typically observed $1/\kappa_l - 1/L$ relation and linear correlation of data; diamond and circle symbols represent GNR and CNT, respectively.

In both SLG and CNT, phonons do not experience boundary scattering in directions perpendicular to the heat flow. Therefore, curvature is possibly responsible for the diameter dependence and lower-than-graphene κ_l value of CNT. On the other hand, CNTs with smaller diameter have less number of optical phonon modes available for phonon scattering, which will lead to longer phonon relaxation times and complicate the diameter dependence. To clarify the role of curvature, we create an artificial boundary in CNT through fixing a row of atoms along the axial direction (fx-CNT), as shown in Fig. 1. Then, fx-CNT, half-rolled GNR (h-GNR), and GNRs with fixed edges (fx-GNR) are constructed through unrolling. These systems are topologically similar and have the same number of optical phonon modes. Therefore, any observed difference in the thermal conductivity among them should be mainly attributed to curvature.

As indicated by the arrows in Fig. 3, the thermal conductivity always monotonically drops from fx-GNR to fx-CNT for all diameters. Since κ_l in classical simulation is proportional to group velocity v_g and relaxation time τ, either of them should be responsible for this reduction in κ_l. Instead of evaluating τ directly from MD through spectral analysis,[14] we perform lattice dynamics calculations for a (5,5) CNT

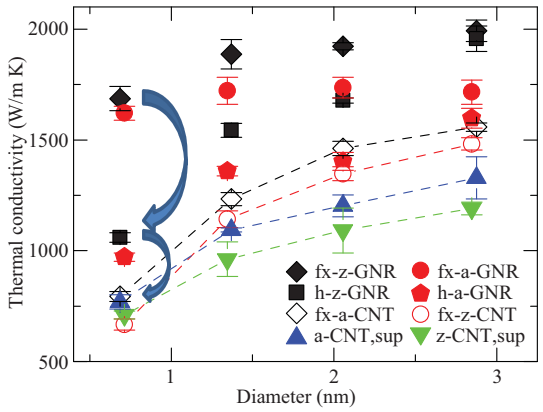

FIG. 3. Extrapolated thermal conductivity of fx-GNR, h-GNR, fx-CNT, and CNT supported on SiO_2 substrate (indicated by the postfix ",sup").

and corresponding GNR to obtain v_g. Under Debye approximation for phonon dispersion, we compute the effective group velocities[33] to be 10.5 km/s for (5,5) CNT, which is larger than 3.2 km/s for corresponding GNR. Recall the lower κ_l of CNT and the above-mentioned proportionality, the stronger curvature of CNT is thus found to shorten the phonon relaxation time. These arguments can also be applied to CNTs with different diameters. Therefore, in free-standing CNTs, the diameter dependence is mainly due to the change in curvature and the number of optical phonon modes,[28] which are competing.

On the other hand, as seen in Fig. 2, κ_l of free-standing a-CNT and z-CNT with similar diameters differ little while that of a-GNR is much lower than that of zigzag ones, agreeing with previous theories.[11,31] In contrast, we find that κ_l of fx-a-CNTs is larger than that of fx-z-CNTs for all diameters, as shown in Fig. 3. This suggests the radial boundary introduces non-negligible chirality dependent phonon scattering into CNT, as opposed to that in free-standing CNTs. A physical system where such chirality dependence may be observed is supported CNT.

In Fig. 3 we show κ_l of a-CNTs and z-CNTs on SiO_2 substrate. When CNT is supported, phonons in CNT experience scattering at CNT-SiO_2 interface with shortened relaxation time.[16] Consistent with the observations on fx-CNTs, we find κ_l of supported a-CNT to be around 10% larger than that of supported z-CNT for all diameters. This indicates interfacial scattering is stronger in supported z-CNTs. Such observation suggests that the chirality dependence of κ_l of supported CNT is due to the chirality dependent phonon boundary scattering rate at CNT-substrate interfaces, which can be roughly modeled as $\tau_b^{-1} = v_g/\pi D$. This is similar to that in fx-CNT and GNR, where boundary scattering or edge localization[11] is also chirality dependent. To verify such dependence experimentally, CNT bundles with single chirality need to be prepared. Despite the great challenges, several groups have managed to produce high concentration CNTs of single chirality.[34,35] With an aligned array of CNTs of single chirality, thermal measurements of their thermal conductivity may be feasible.

As compared to κ_l values of free-standing CNTs in Fig. 2, we observe reduction in κ_l of around 34% and 41% for supported a-CNT and z-CNT, respectively. Such reduction is mainly due to the shortened phonon relaxation time instead of group velocity.[14] Nonetheless, the observed reduction is less than that in supported graphene, considering its drop in κ_l from $\sim$2500 W/mK (Ref. 36) to $\sim$600 W/m K (Ref. 13) (76%) at room temperature. The alleviated thermal conductivity reduction can be due to the fact that the atomic vibrations of a smaller fraction of carbon atoms in supported CNT are perturbed than in the case of supported graphene.[13] Therefore, aligned CNT array may have better thermal conductance than SLG when supported.

In summary, we used NEMD simulations to study the thermal conductivity of free-standing and supported CNT as well as free-standing GNR/SLG with 0.7 to 2.9 nm diameter and armchair/zigzag chiralities. Our main findings are (1) the thermal conductivity of free-standing CNT increases with diameter and approaches that of SLG asymptotically, owing to curvature that shortens phonon relaxation time; (2) the thermal conductivity of supported a-CNT is about 10% larger than that of z-CNT of similar diameter due to chirality dependent phonon scattering at CNT-substrate interface; and (3) the thermal conductivity reduces by around 34%-41% when CNT is supported on SiO_2 substrate, less than that found in supported SLG.

This work is supported by the Air Force Office of Scientific Research (AFOSR) through the Discovery Challenge Thrust (DCT) Program (Grant FA9550-11-1-0057, Program Manager Joan Fuller) and by the Cooling Technologies Research Center (CTRC), an NSF University/Industry Cooperation Research Center. B. Qiu thanks Li Shi for insightful discussions.

[1]A. K. Geim and K. S. Novoselov, Nature Mater. **6**, 183 (2007).
[2]A. A. Balandin, Nature Mater. **10**, 569 (2011).
[3]J. S. Soares, A. P. M. Barboza, P. T. Araujo, N. M. B. Neto, D. Nakabayashi, N. Shadmi, T. S. Yarden, A. Ismach, N. Geblinger, E. Joselevich *et al.*, Nano Lett. **10**, 5043 (2010).
[4]D. Donadio and G. Galli, Phys. Rev. Lett. **102**, 195901 (2009).
[5]J. Shiomi and S. Maruyama, Phys. Rev. B **73**, 205420 (2006).
[6]D. V. Kosynkin, A. L. Higginbotham, A. Sinitskii, J. R. Lomeda, A. Dimiev, B. K. Price, and J. M. Tour, Nature **458**, 872 (2009).
[7]S. J. Tans, M. H. Devoret, H. Dai, A. Thess, R. A. Smalley, L. J. Geerlgs, and C. Dekker, Nature **386**, 474 (1997).
[8]H. Zhao, K. Min, and N. R. Aluru, Nano Lett. **9**, 3012 (2009).
[9]A. Naeemi and J. D. Meindl, IEEE Electron Device Lett. **28**, 428 (2007).
[10]Y. Xu, X. Chen, B.-L. Gu, and W. Duan, Appl. Phys. Lett. **95**, 233116 (2009).
[11]Y. Wang, B. Qiu, and X. Ruan, "Edge effect on thermal transport in graphene nanoribbons: a phonon localization mechanism beyond edge roughness scattering" (unpublished).
[12]M. A. Osman and D. Srivastava, Nanotechnology **12**, 21 (2001).
[13]J. H. Seol, I. Jo, A. L. Moore, L. Lindsay, Z. H. Aitken, M. T. Pettes, X. Li, Z. Yao, R. Huang, D. Broido *et al.*, Science **328**, 213 (2010).
[14]B. Qiu and X. Ruan, Appl. Phys. Lett. **100**, 193101 (2012).
[15]Z. Y. Ong and E. Pop, Phys. Rev. B **84**, 075471 (2011).
[16]Z. Y. Ong, E. Pop, and J. Shiomi, Phys. Rev. B **84**, 165418 (2011).
[17]A. V. Savin, B. Hu, and Y. S. Kivshar, Phys. Rev. B **80**, 195423 (2009).
[18]T. Yamamoto, S. Watanabe, and K. Watanabe, Phys. Rev. Lett. **92**, 075502 (2004).
[19]S. Plimpton, J. Comput. Phys. **117**, 1 (1995).
[20]L. Lindsay and D. A. Broido, Phys. Rev. B **81**, 205441 (2010).
[21]S. Munetoh, T. Motooka, K. Moriguchi, and A. Shintani, Comput. Mater. Sci. **39**, 334 (2007).
[22]T. Hertel, R. E. Walkup, and P. Avouris, Phys. Rev. B **58**, 13870 (1998).
[23]A. K. Rappe, C. J. Casewit, K. S. Colwell, W. A. Goddard, and W. M. Skiff, J. Am. Chem. Soc. **114**, 10024 (1992).
[24]Z. Huang and Z. Tang, Physica B **373**, 291 (2006).
[25]Z. Y. Ong and E. Pop, Phys. Rev. B **81**, 155408 (2010).

[26]A. Bagri, S.-P. Kim, R. S. Ruoff, and V. B. Shenoy, Nano Lett. **11**, 3917 (2011).
[27]P. K. Schelling, S. R. Phillpot, and P. Keblinski, Phys. Rev. B **65**, 144306 (2002).
[28]J. A. Thomas, J. E. Turney, R. M. Iutzi, C. H. Amon, and A. J. H. McGaughey, Phys. Rev. B **81**, 081411 (2010).
[29]G. Zhang and B. Li, J. Chem. Phys. **123**, 114714 (2005).
[30]J. Shiomi and S. Maruyama, Jpn. J. Appl. Phys., Part 1 **47**, 2005 (2008).
[31]L. Lindsay, D. A. Broido, and N. Mingo, Phys. Rev. B **82**, 161402(R) (2010).
[32]J. Tersoff, Phys. Rev. Lett. **61**, 2879 (1988).
[33]J. Hu, X. Ruan, and Y. P. Chen, Nano Lett. **9**, 2730 (2009).
[34]A. Vijayaraghavan, F. Hennrich, N. Sturzl, M. Engel, M. Ganzhorn, M. Oron-Carl, C. W. Marquardt, S. Dehm, S. Lebedkin, M. M. Kappes *et al.*, Acs Nano **4**, 2748 (2010).
[35]H. Liu, D. Nishide, T. Tanaka, and H. Kataura, Nature Commun. **2**, 309 (2011).
[36]W. Cai, A. L. Moore, Y. Zhu, X. Li, S. Chen, L. Shi, and R. S. Ruoff, Nano Lett. **10**, 1645 (2010).